



ESTIMATION OF ANCHORAGE STRENGTH THROUGH BENDING SHEAR TESTS ON RC BEAMS WITH SECOND-LAYER BARS CUT OFF

Y. Shinohara¹⁾

⁽¹⁾ Associate Professor, Laboratory for Future Interdisciplinary Research of Science and Technology, Division of Structural Engineering (formerly SERC), Tokyo Institute of Technology, shinohara.y.ab@m.titech.ac.jp

Abstract

The amount of reinforcement required in a reinforced concrete building has increased due to the increased demand for high-rises and advanced seismic performance. In particular, the amount of reinforcement required at the ends of a beam has increased, and the reinforcement tends to be arranged in multiple stages, where the second-layer reinforcement is frequently cut off at the central part of the beam. However, since there have been few studies on the bond behavior of cut-off longitudinal reinforcements, the bond strength based on the effective bond length is not evaluated appropriately, and it is difficult to design the cut-off reinforcement with a rational anchorage length. Experiments were conducted on the reinforced concrete beam arranged with second-layer bars cut off in order to study the influence of the bond reinforcement on the bond-splitting strength or anchorage behaviors. The longitudinal bars were reinforced with transverse bars having different configurations (separated and closed types) and strengths ($\sigma_y=295$ and 1275 N/mm²). The bond strength of the second-layer bars reinforced by separated-type bars was almost equal to the strength of those reinforced by closed-type bars. High-strength bond reinforcement increased the bond strength by 30%. The test results also showed that the bond strength of the second-layer cut-off bars was considerably higher than the calculated value based on the AIJ design guidelines. A new reduction coefficient for the second-layer cut-off bars was proposed to reasonably estimate the bond strength for anchorage failure.

Keywords: Bond-splitting behavior, Cut-off bar, Second-layer bar, Bond reinforcement, Reduction coefficient

1. Introduction

In recent years, the amount of reinforcement required in a reinforced concrete (RC) building has increased due to the increased demand for high-rises and advanced seismic performance. Also, an overcrowded bar arrangement has an adverse influence on the bar arrangement design of an RC building. In particular, the amount of reinforcement required at the end of a beam increases, and the reinforcement tends to be arranged in multiple stage. Because the bending moment in an RC beam generally declines toward the midsection when a seismic load is applied, the reinforcement is frequently cut in the central part of the beam, and the cut-off reinforcement is also advantageous from the precast construction viewpoint. In a multistage-type bar arrangement, since the bond strength of the second-layer longitudinal reinforcement is adversely affected by the bond behavior of the first-layer longitudinal reinforcement, the bond strength between the reinforcement and the concrete decreases. The bond strength of the second-layer longitudinal reinforcement is reduced by 0.6 times the first-layer longitudinal reinforcement in accordance with the Design Guidelines for Earthquake Resistant RC Buildings Based on Inelastic Displacement Concept [1] (hereinafter referred to as the guideline equation). Since it is necessary to transmit stress by a short bond length when the second-layer longitudinal reinforcement is cut off, the danger of bond-splitting or anchorage failure increases. Moreover, when dissolving an overcrowded bar arrangement with high-strength reinforcement for lateral reinforcements, a reduction in the amount of reinforcement can easily decrease the bond-splitting strength or cause anchorage failure.

However, since there has been little research on the bond behavior of cut-off longitudinal reinforcement, the bond strength based on the effective bond length of a cut-off reinforcement has not yet been evaluated appropriately, and it is difficult to design the cut-off reinforcement with a rational anchorage length according to the guideline equation [2, 3]. Therefore, in this paper, in order to study the effects of various lateral reinforcements on the bond behavior and crack pattern of the second-layer cut-off longitudinal reinforcement, an experiment was conducted on RC beam specimens with two-layer longitudinal reinforcements. The experimental



parameters are the diameter of the longitudinal reinforcement, the basic high-strength shear reinforcement ratio, the cut-off length, the concrete strength and the amount, configuration, and strength of the bond reinforcement. The allowance of the design equation for the bond strength is evaluated and investigated by comparing the experimental value and guideline equation using various bond reinforcements. The main purpose of this research is to propose a simple and reasonable bond-strength reduction coefficient for bond/anchorage failure of the second-layer cut-off longitudinal reinforcement based on those experimental results and considerations.

2. Bond experimental method for RC beams having second-layer bars cut off

2.1 Specimen details

The specimen details used for the experiment are shown in Table 1. The RC beam specimens are one-half scale models, and the common factors are the cross-sectional dimensions (350 mm × 500 mm) and the test section length (2550 mm and a shear span ratio of about 3). The diameter and the number of longitudinal reinforcements are the same in the first and second layers, that is, 4-D25 for Series 1 and 4-D22 for Series 2 arranged in two layers. The value following the first S of the specimen name is the high-strength shear reinforcement ratio (%). The value following the C or the second S indicates the bond reinforcement ratio (%). C and S are abbreviations for closed and separated, respectively, and they express the bond reinforcement configuration (Fig. 1). Furthermore, U indicates high-strength reinforcement. The last character expresses the cut-off length, where M is 1070 mm, and S is 970 mm. The cut-off length was determined such that it satisfies the length specified in the AIJ bar-arrangement guideline [4], that is, $l_0/4+15d$, where l_0 is the clear span of the beam, and d is the diameter of the longitudinal reinforcement. However, the last character Fc indicates the concrete strength (Fc27), while the others are Fc39.

As shown in Table 2, the mix-design strengths of concrete are Fc39 and Fc27, but since the compressive strength changes with the batch of concrete and the different dates of loading, the compressive strength of each specimen calculated by the linear interpolation is also shown in Table 1. The concrete was placed laterally in order to avoid the difference in bond strength between the top reinforcement and bottom reinforcement due to bleeding.

Table 1 – List of test specimens, calculated strengths, and test results

Series	Test designation	Compressive strength (N/mm ²)	Cut-off length (mm)	Shear transverse rebar	Bond transverse rebar	Bond strength from design guidelines		Strength from design guidelines		Strength from sectional analysis		Test results (kN)	
						τ_{1cal} (N/mm ²)	τ_{2cal} (N/mm ²)	Q _{SU} (kN)	Q _{BU} (kN)	Q _{2BU} (kN)	Q _{FU} (kN)		
1 4-D25 $p_r=0.27\%$	S0.6-M	44.7	1070	U10.7 @85 mm $p_w=0.6\%$	—	4.6	3.1	1057	1049	401	876	798	
	S0.6+C0.11-M	44.9			D6 $p_{wb}=0.11\%$	5.6	3.4	1058	1201	437	878	837	
	S0.6+C0.24-M	45.1			D10 $p_{wb}=0.24\%$	6.2	3.7	1062	1308	480	878	930	
	S0.6+S0.24-M	45.2				6.2	3.7	1063	1309	480	879	917	
	S0.6+C0.24-Fc	30.0				5.7	3.4	818	1182	446	786	738	
	S0.6+US0.13-M	43.2			U7.1 $p_{wb}=0.13\%$	5.7	3.4	1036	1210	471	890	891	
2 4-D22 $p_r=0.21\%$	S0.3-M	38.3	1070	U7.1 @80 mm $p_w=0.3\%$	—	3.8	2.5	864	657	292	763	472	
	S0.3+C0.29-M	46.7			D10 $p_{wb}=0.29\%$	5.8	3.5	941	921	417	819	698	
	S0.3+C0.58-M	42.4			D10 $p_{wb}=0.51\%$	7.1	4.2	904	1079	499	798	817	
	S0.3+US0.29-S	38.5			970	U7.1 $p_{wb}=0.29\%$	4.9	3.3	871	981	335	744	785
	S0.3+US0.51-S	39.6				U10.7 $p_{wb}=0.51\%$	6.7	4.0	882	1235	405	754	855

Note: Design guideline indicated by Earthquake Resistant Reinforced Concrete Buildings Based on Inelastic Displacement Concept [1]

τ_{1cal} and τ_{2cal} : Bond strength of 1st and 2nd layer longitudinal bar from AIJ design guideline [1]/0.8

Q_{SU} and Q_{BU}: Shear capacity and bond-splitting capacity from AIJ design guideline [1]

Q_{2BU}: Bond capacity of 2nd layer longitudinal bars based on sectional analysis

Q_{FU}: Flexural capacity based on sectional analysis when $\epsilon_{cu}=0.3\%$



The mechanical properties of the reinforcement arranged in the specimens are shown in Table 3. Since the main purpose of this experiment is to investigate the bond strength, the specimen should have bond-splitting failure before flexural yield. For this reason, all of the longitudinal-reinforcement SD390 used for the specimen had an increased strength of up to about 1000 N/mm² by hardening (see Table 3). All of the fundamental shear reinforcements are high-strength reinforcement SBPD1275, and U10.7 (@85 mm, $\sigma_y=1380$ N/mm², $p_w = 0.6\%$) is used in the Series 1 specimen and U7.1 (@80 mm, $\sigma_y=1454$ N/mm², and $p_w = 0.3\%$) in the Series 2 specimen. As shown in Fig. 1, the bond reinforcements of the closed-type (C) and separated-type (S) configurations are further added to the basic specimens S0.6-M and S0.3-M, which were not arranged with bond reinforcement.

Moreover, two types of bond reinforcement strengths, normal-strength reinforcement SD295 (C, S) and high-strength reinforcement SBPD1275 (U), are used to study the effect of the reinforcement strength on the bond-splitting failure. The bond strengths (τ_{1cal} and τ_{2cal}) of the first- and second-layer longitudinal reinforcements obtained by the guideline equation are also shown in Table 1. Since the guideline equation for the bond strength adopts the lower limit of the experimental results by multiplying the mean values of the previous experimental results by 0.8, the bond strength in Table 1 is restored to the experiment mean value by dividing by 0.8 to compare with these test results. Q_{SU} in Table 1 is the shear strength according to the guideline

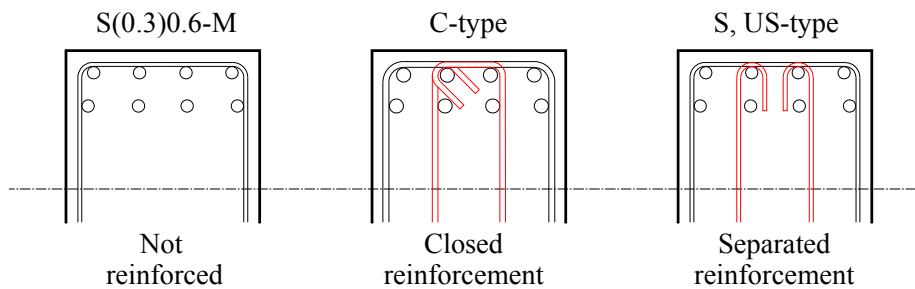


Fig. 1 Configurations of bond reinforcement

Table 2 – Mix proportions of concrete (Unit: kg/m³)

Nominal strength	W/C	Water	Cement	Sand	Aggregate	Admixture
Fc39	0.50	180	360	656	979	3.60
Fc27	0.60	190	317	623	976	3.17

Table 3 – Mechanical properties of reinforcement

Designation	σ_y (N/mm ²)	σ_B (N/mm ²)	E_s (10 ⁵ N/mm ²)	ϵ_y (μ)
Long. bar: D25	955	1093	1.82	5699
Long. bar: D22	974	1093	1.79	5834
Trans. bar: D6	277	532	1.62	1768
Trans. bar: D10	368	521	1.59	2581
Trans. bar: U7.1	1454	1483	1.88	7735
Trans. bar: U10.7	1373	1492	1.94	7294

σ_y : Yield strength, σ_B : Tensile strength, E_s : Young's modulus, ϵ_y : Strain at yield strength



equation, and Q_{BU} is the shear strength considering the effect of the bond failure. Furthermore, Q_{2BU} is the bond strength of the second-layer longitudinal reinforcement, and Q_{FU} shows the flexural strength when the compression edge reaches the ultimate strain ($\epsilon_{cu} = 0.3\%$) of the concrete.

2.2 Loading and measurement method

An example of the strain gauge location on the reinforcement is shown in Fig. 2. As for the longitudinal reinforcements, the strains of only two reinforcements (the third from the bottom and the bottom in casting) were measured out of the four reinforcements arranged in the width direction. The strain of the longitudinal reinforcement, which is in tension for positive loading, was measured at intervals of 160 mm in addition to two points at 210 mm intervals from the member edge to investigate the bond behavior. Specifically, regarding the strain measurement of the second-layer longitudinal reinforcement, two strain gauges were attached at one point for the important section from the member end to 420 mm (equal to effective depth), and the mean value was used. All of the strain gauges on the longitudinal reinforcement were attached on the side of the reinforcement so that it would not be affected by the flexural deformation. In order to minimize the strain gauge's effect on the bond properties, a small strain gauge with a gauge length of 2 mm (base length of 5.5 mm) was used, and the lead wire was laid 100 mm from the inner side of the reinforcement. As for the shear reinforcement and the bond-splitting reinforcement, the strains in the center of the reinforcement near the bottom in casting were measured to evaluate the bond reinforcing bars, which control bond-splitting cracks.

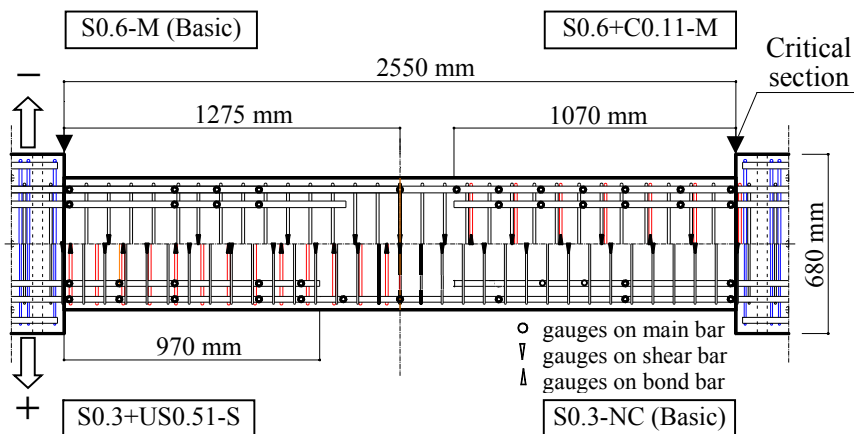


Fig. 2 Locations of strain gages attached on bars

The loading device is shown in Fig. 3. The right stub of the specimen was firmly connected to the loading frame with high-strength steel bars. The left stub of the specimen was connected with a loading beam that had a crank for restraining the deformation of the surface outside the beam. After installing the 1000 kN and 500 kN hydraulic jacks on the loading beam, cyclic loading was performed by displacement control using two jacks with a controller so that the left stub did not rotate and so that double curvatures resulted in the specimen. The displacement was decreased when the rotation angle of the beam amounted to $\pm 1/400$ (1 cycle), and $\pm 1/200$, $\pm 1/100$, $\pm 1/50$, and $\pm 1/33$ (2 cycles) until peak loading. However, the loading was stopped when the shear force of the first cycle did not exceed the previous maximum value. The relative displacement (horizontal and vertical) between the stubs was measured using jigs attached to the right and left stubs. The crack was also measured using a digital microscope with a resolution of 0.01 mm.

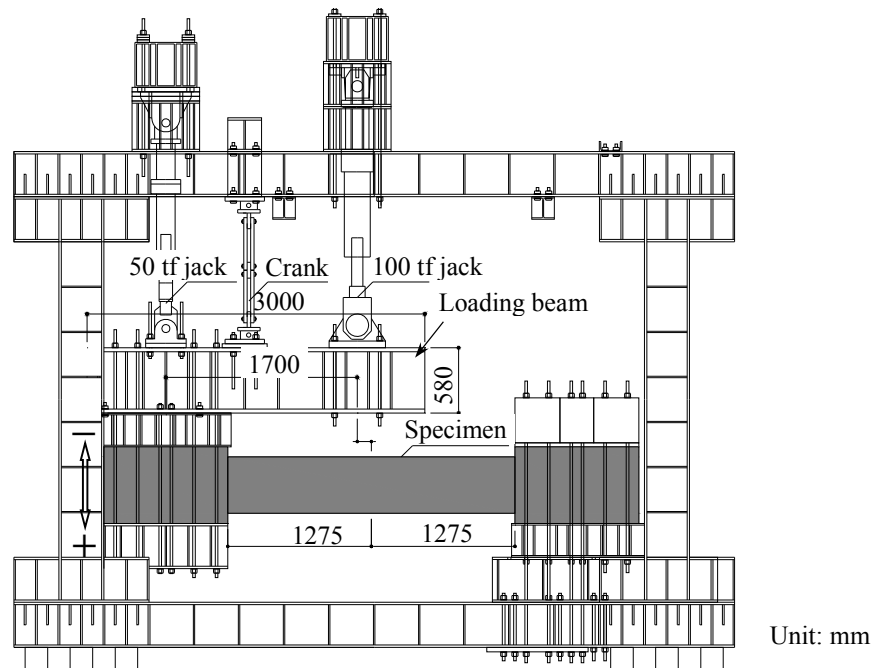


Fig. 3 Loading apparatus adapted to produce double curvatures

3. Experimental results and discussion

3.1 Relationship between shear force and rotation angle

Fig. 4 shows the relationship between the shear force Q and rotation angle R obtained from the experiment. The bond (anchorage) strength Q_{2BU} of the second-layer longitudinal reinforcement and the flexural strength Q_{FU} of the beam specimen shown in Table 1 are also drawn on the figure with a broken line and a long-dashed short-dashed line, respectively. The circle in the figure shows the maximum strength, and the square shows the yield of the first-layer longitudinal reinforcement. Moreover, the triangle is the maximum average bond stress of the second-layer longitudinal reinforcement, and the diamond is the maximum partial bond stress for the second-layer longitudinal-reinforcement tip section.

As shown in Table 4, the shear reinforcement and the bond-splitting reinforcement using high-strength reinforcement did not yield throughout the loading. On the other hand, most normal-strength bond-splitting reinforcements resulted in yield at the maximum strength of the beam specimen. Regarding the failure mode, since the bond stress of the second-layer cut-off longitudinal reinforcement reached the maximum value before the maximum strength of the beam specimen, it is concluded that all of the specimens would have bond-splitting failure as planned.

Specimens S0.3+US0.29-S and S0.3+US0.51-S, which have longitudinal reinforcement D22 and high-strength bond-splitting reinforcement, resulted in flexural failure accompanied by bond deterioration of the second-layer longitudinal reinforcement. Since specimen S0.6+S0.24-M (separated-type bond reinforcement) and specimen S0.6+C0.24-M (closed-type bond reinforcement) had almost the same relationship between the shear force and rotation angle, when a separated-type bond reinforcement is continuous between the top and bottom longitudinal reinforcement, it is expected that a separated type has a reinforcement effect equivalent to a closed type.

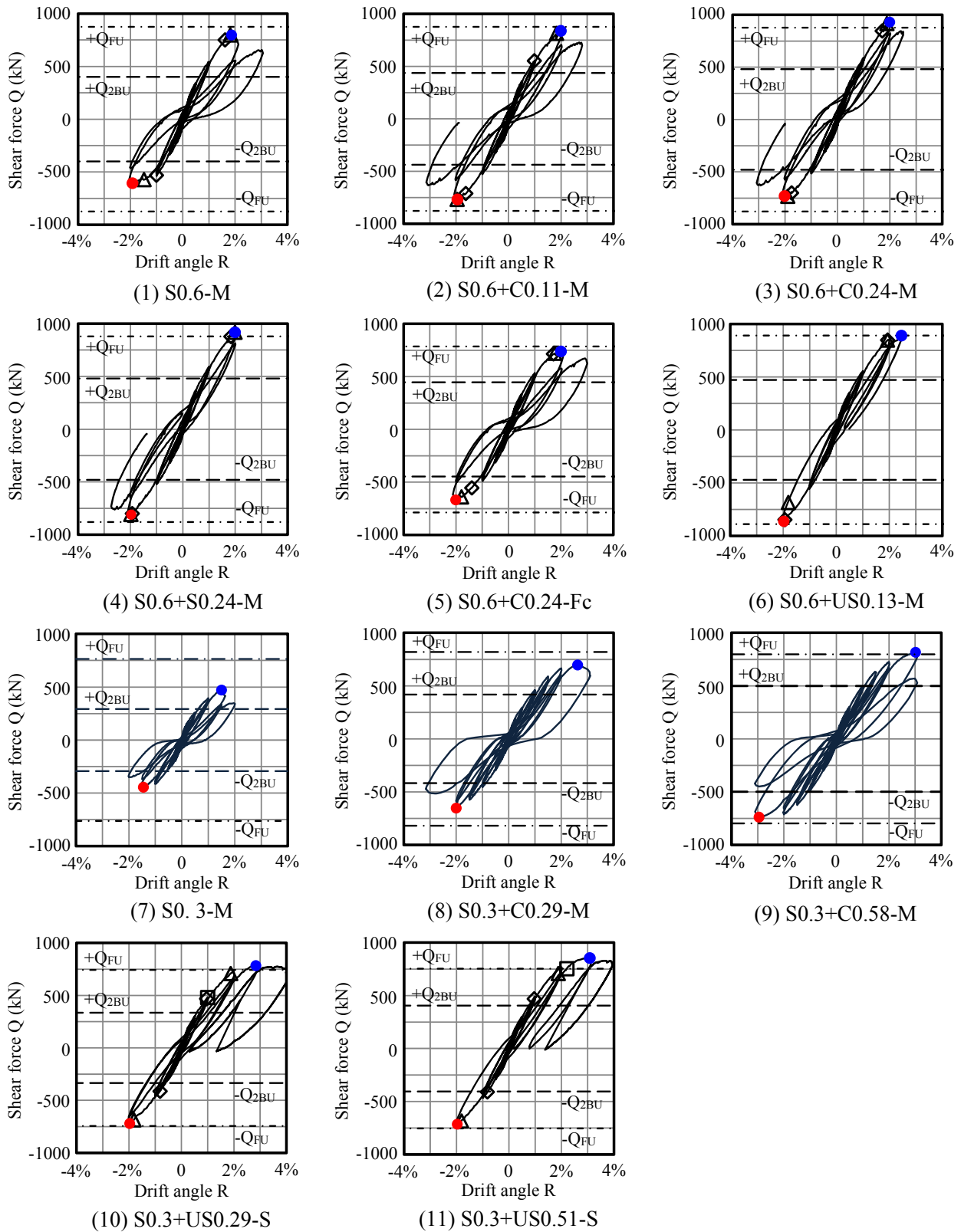


Fig. 4 Comparisons of Q-R curves and typical capacities



Table 4 Stresses in each transverse bar at maximum shear force (N/mm²)

Specimen designation	Transverse bar	Order from center to right(+) and left(-)							
		-4	-3	-2	-1	+1	+2	+3	+4
S0.6-M	shear	361	590	643	442	299	456	446	238
S0.6+C0.11-M	shear	139	586	650	505	326	478	422	26
	bond	<u>277</u>	<u>277</u>	<u>277</u>	 	 	<u>277</u>	<u>277</u>	<u>277</u>
S0.6+C0.24-M	shear	238	401	833	420	270	559	441	216
	bond	308	<u>368</u>	324	 	 	***	224	<u>368</u>
S0.6+S0.24-M	shear	214	393	539	331	288	372	375	144
	bond	361	300	<u>368</u>	 	 	***	218	<u>368</u>
S0.6+C0.24-Fc	shear	309	386	610	365	368	485	354	180
	bond	<u>368</u>	<u>368</u>	<u>368</u>	 	 	355	298	<u>368</u>
S0.6+US0.13-M	shear	383	742	608	413	473	525	656	386
	bond	507	980	764	565	487	597	776	707
S0.3-M	shear	633	815	910	434	577	1138	642	550
S0.3+C0.29-M	shear	959	979	1275	630	816	****	938	1041
	bond	<u>374</u>	****	****	 	 	331	<u>374</u>	357
S0.3+C0.58-M	shear	894	681	834	569	693	1263	1171	1004
	bond	122	<u>374</u>	81	 	 	<u>374</u>	317	250
S0.3+US0.29-S	shear	602	910	798	513	592	879	997	531
	bond	882	805	865	590	678	815	905	752
S0.3+US0.51-S	shear	726	700	704	440	543	811	767	611
	bond	514	635	512	453	512	453	662	470

Underlined: At or above yield strength

****: Not measured due to strain gauge damage

3.2 Crack pattern and failure mode

Typical crack patterns at the maximum shear loads of the beam specimens are shown in Fig. 5 with a crack trace (upper) and photograph (lower). As for specimens S0.6-M and S0.6+C0.24-M, which had bond-splitting failure, the bond-splitting crack appeared clearly along the longitudinal reinforcement. Regarding the bond-splitting crack behavior, the first crack generated near the tip of the second-layer cut-off longitudinal reinforcement progressed in the diagonal direction under the effect of the shear force. Simultaneously, another bond-splitting crack was induced along the first-layer longitudinal reinforcement in the center of the specimen. Finally, the damage increased remarkably near the tip of the cut-off reinforcement. It is supposed that this damage was caused by the high bond stress, as shown in the following section. On the other hand, specimens S0.6+US0.13-M and S0.3+US0.29-S, which had high-strength bond reinforcement, reached the final maximum strength by flexural failure after the bond deterioration of the second-layer cut-off reinforcement. For that reason, most of the compression-side cover concrete fell off in the critical cross section, and the bond-splitting crack in the center of the beam specimen did not significantly increase. If the amount of the bond reinforcement is similar in Table 4, the stress in the high-strength bond reinforcement (-US-) increased to more than twice as much as that of the normal-strength reinforcement (C or S); as a result, high-strength bond reinforcement was more effective against bond-splitting cracks.

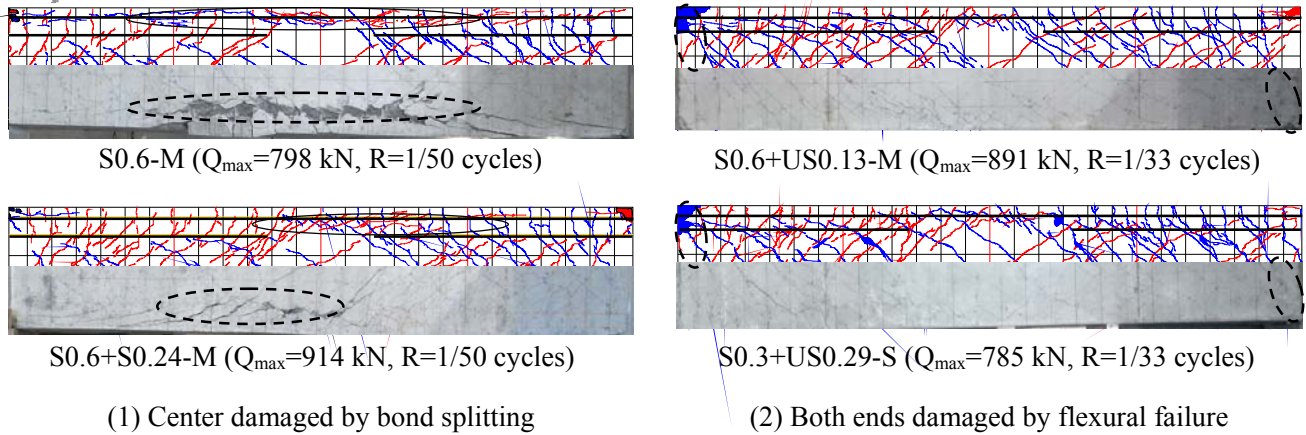


Fig. 5 Typical crack patterns at maximum shear loads of beam specimens and photos after loading

3.3 Strain distributions of longitudinal reinforcement

The typical strain distributions in positive loading are shown in Fig. 6 for the first and second layers of the top longitudinal reinforcement. Although the strain was measured for the first- and second-layer longitudinal reinforcements arranged inside and outside, the mean values are shown in the figure. The strain distribution of the bottom reinforcement was mostly antisymmetric. The solid line is the strain distribution of the second-layer

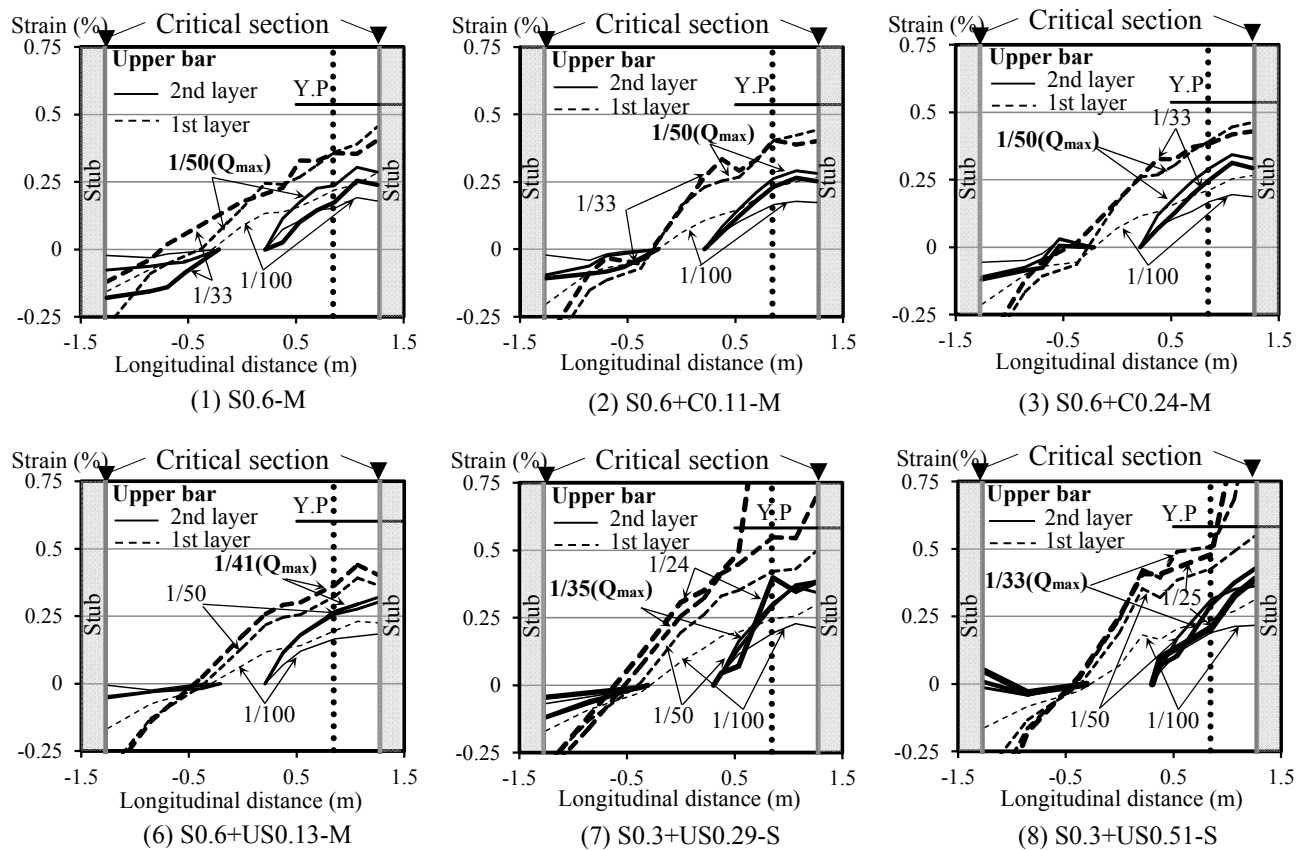


Fig. 6 Transition of strain distributions in top longitudinal reinforcement under positive cycles



longitudinal reinforcement, the dashed line is the strain distribution of the first-layer longitudinal reinforcement, and the dotted line shows the location of the effective depth d ($= 430$ mm) from the tension side of the critical cross section. Moreover, the number in the figure is the rotation angle R , and the strain distributions after $R=1/100$ are shown.

If paying attention to the second-layer cut-off longitudinal reinforcement, the variation in the strain distribution on the compression side was smaller than that on the tension side, and the strain slope (bond stress) at the tip of the tension side was the largest up to the maximum strength of the beam. As for the specimen with normal-strength bond reinforcement (top of Fig. 6), since the strain slope at the tip of the cut-off decreased, the bond can be expected to have deteriorated before and behind the maximum strength. The strain slope of the first-layer longitudinal reinforcement of all the specimens maintained a slope almost comparable to the rotation angle after the maximum strength. Also, the strain slope was not uniform across the overall length, that is, a steep slope in the cut-off part of the second-layer longitudinal reinforcement and a gradual slope from the critical cross section to the effective depth due to the tension shift. On the other hand, since the strain slope of the second-layer cut-off longitudinal reinforcement decreased before and behind the maximum strength of the beam specimen, the bond deterioration of the second-layer cut-off longitudinal reinforcement occurred earlier than for the first-layer longitudinal reinforcement.

3.4 Maximum average bond stress

The maximum average bond stress of each longitudinal reinforcement for positive loading is shown in Table 6. The calculated value is the mean experimental value, in which the guideline equation value is divided by 0.8. Since a strain shift was observed on the tension side, as shown in Fig. 7, the average bond stress of the first-layer longitudinal reinforcement was calculated using the strain separated from the critical cross section on the tension side by 420 mm and the strain of the critical cross section on the compression side. The average bond stress of the second-layer cut-off reinforcement was calculated by setting the strain of the cut-off tip to 0.

The numerical values in the table are the maximum values of the average bond stress for each longitudinal reinforcement, and the rotation angle for each maximum bond stress may be different in the same specimen. The

Table 6 List of maximum average bond stresses at positive loading

Specimen	Calculation (N/mm ²)		Maximum average bond stress (N/mm ²)							
	τ_{1cal}	τ_{2cal}	Upper 1st		Upper 2nd		Lower 1st		Lower 2nd	
			In	Out	In	Out	In	Out	In	Out
S0.6-M	4.6	3.1	3.0	<u>3.6</u>	3.9	<u>4.8</u>	3.5	<u>4.3</u>	4.5	5.4
S0.6+C0.11-M	5.6	3.4	2.0	4.1	4.6	5.1	4.1	4.6	4.1	5.0
S0.6+C0.24-M	6.2	3.7	4.0	4.3	5.0	5.5	4.7	4.5	6.4	5.7
S0.6+S0.24-M	6.2	3.7	<u>4.3</u>	<u>4.7</u>	5.1	5.6	<u>4.8</u>	3.9	5.6	5.1
S0.6+C0.24-Fc	5.7	3.4	3.6	<u>4.0</u>	4.3	4.6	3.3	3.5	4.2	4.8
S0.6+US0.13-M	5.7	3.4	3.1	4.5	4.5	4.7	4.0	4.0	5.8	<u>4.9</u>
S0.3-M	3.8	2.5	2.2	2.5	3.0	3.1	2.2	2.3	3.0	3.0
S0.3+C0.29-M	5.8	3.5	3.7	<u>4.3</u>	4.0	3.9	<u>3.4</u>	<u>3.6</u>	4.0	3.8
S0.3+C0.58-M	7.1	4.2	4.5	5.2	6.3	4.8	4.7	4.4	5.3	4.4
S0.3+US0.29-S	4.9	3.3	<u>4.0</u>	<u>4.5</u>	<u>7.7</u>	5.2	4.0	<u>4.1</u>	7.4	5.6
S0.3+US0.51-S	6.7	4.0	5.1	<u>3.8</u>	8.4	5.2	<u>5.1</u>	<u>4.5</u>	<u>8.0</u>	5.8

τ_{1cal} and τ_{2cal} : Calculated by AIJ design guideline¹/0.8

Bold and underlined: before and after maximum shear force, respectively



bold values in the table are the values before the maximum strength of the beam specimen, and the underlined values are the values after the maximum strength; the other values indicate that the bond stress reached the maximum value at the same time as the maximum strength. Many second-layer cut-off longitudinal reinforcements reached the maximum bond stress before the maximum strength, while many first-layer longitudinal reinforcements reached the maximum bond stress after the maximum strength. Furthermore, the maximum average bond stress of the first-layer longitudinal reinforcement did not reach the previous experimental mean value (guideline equation value/0.8). This may be because the strength of the beam specimen declined due to the first-layer longitudinal reinforcement yielding following the bond deterioration of the second-layer cut-off longitudinal reinforcement. When the bond-splitting reinforcement was arranged inside, the bond stress of the inner-side reinforcement increased further. Especially, the maximum bond stress of the inner-side reinforcement of specimens S0.3+US0.29-S and S0.3+US0.51-S with high-strength bond reinforcement of 0.29% and 0.51% ascended to about 8 N/mm² and increased about 30% as compared with the specimen with the same amount of normal-strength bond reinforcements. Furthermore, it can be seen that the separated-type reinforcement (S) showed a reinforcing effect equivalent to a closed-type reinforcement (C) by comparing specimens S0.6+C0.24-M and S0.6+S0.24-M.

4. Bond/anchorage strength of the second-layer cut-off longitudinal reinforcement

Fig. 7 shows the relationship between the bond strength of the second-layer cut-off longitudinal reinforcement obtained from the test and the bond strength τ_{bu2} (refer to Eq. (1)) of the second-layer longitudinal reinforcement according to the guideline equation. The average allowance (experimental values divided by Eq. (1)) for the design guideline equation of all 11 specimens is 1.81 with a coefficient of variation of 16%, which is considerably high. The bond strength of the second-layer longitudinal reinforcement τ_{bu2} is shown in Eq. (1) in accordance with the design guideline [1],

$$\tau_{bu2} = \alpha_2 * \alpha_t \left\{ (0.085b_{st2} + 0.10) \sqrt{\sigma_B} + k_{st2} \right\} \quad (1)$$

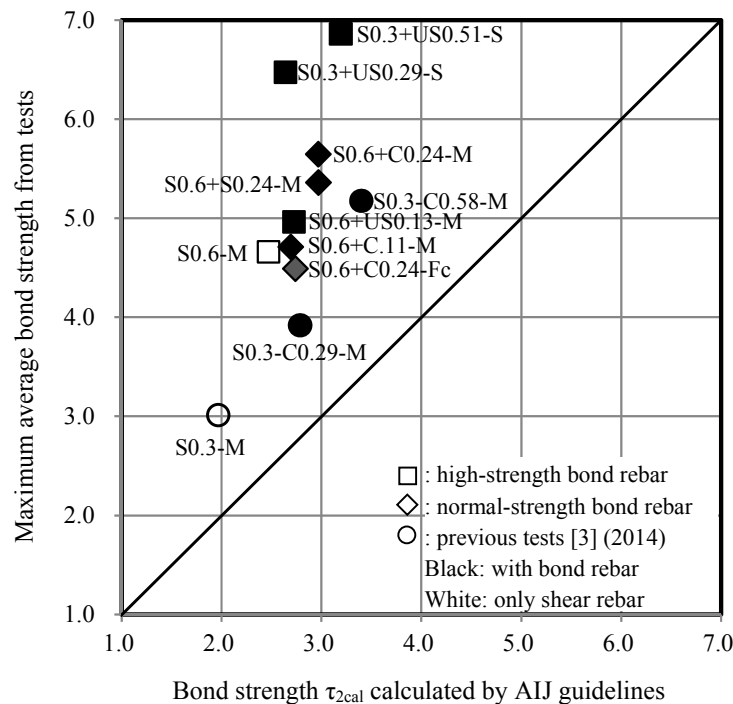


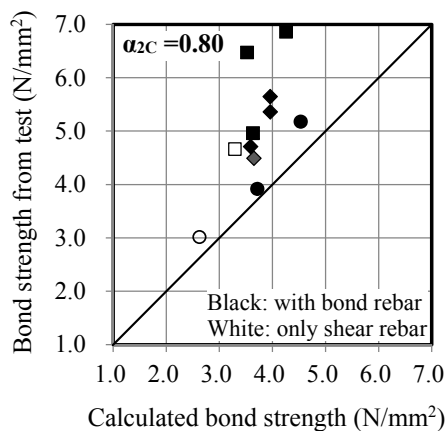
Fig. 7 Comparison of bond strengths between tests and AIJ guidelines



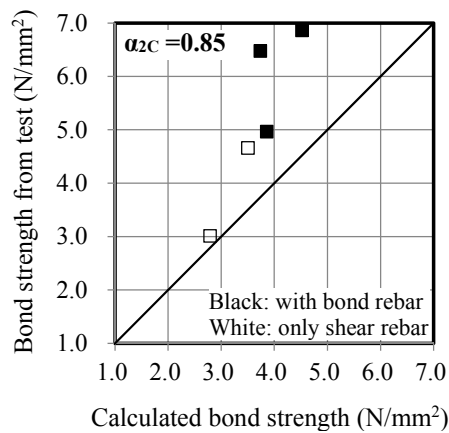
where α_2 ($=0.6$) and α_t are the reduction coefficient for the second-layer longitudinal reinforcement and the top reinforcement, respectively, and $\alpha_t=1$ in this specimen since the concrete was placed laterally, which is perpendicular to the loading.

The present design guideline equation conservatively estimates the bond strength for the second-layer longitudinal reinforcement based on previous experimental data, and the average allowance is 1.38 with a coefficient of variation of 22%. For that reason, the bond strength proposed for the second-layer cut-off longitudinal reinforcement should have an equivalent average allowance and coefficient of variation. Generally, the bond strength is strongly affected by the ratio of the first- and second-layer reinforcements and the influence of the effective bond length. In this investigation, the specimen with the same numbers of first- and second-layer reinforcements (generally the minimum bond strength) and a cut-off length according to the AIJ code [4] (more than $l_0/4+15d$, where l_0 is the clear span and d is the diameter of a bar) is reviewed in order to propose a relevant bond-strength equation. Since the present design bond strength of the second-layer cut-off longitudinal reinforcement is underestimated, it is possible to easily obtain the practical bond strength for the cut-off reinforcement by increasing the reduction coefficient α_2 ($=0.6$) in Eq.(1).

The relationship between the experimental bond strength result for all 11 specimens and the calculated bond strength, which increased the reduction coefficient α_2 to 0.8, is shown in Fig. 8(a). Since all of the specimens are considered safe and the average allowance is 1.35 with a coefficient of variation of 16%, a reliable strength equation equivalent to the present guideline equation is obtained. Moreover, unless the bond reinforcement yields, the reinforcing effect increases due to the high confinement of the bond-splitting crack. Therefore, when the bond reinforcement does not yield, it is possible to increase α_2 further. Regarding the five specimens with high-strength bond reinforcement, the experimental results for the bond strength calculated as $\alpha_2=0.85$ are shown in Fig. 8(b). Although there are only five specimens, all are considered safe, and the average allowance is 1.39 with a coefficient of variation of 16%; thus, the reliability is equivalent to the value obtained using the present strength equation.



(a) All 11 specimens



(b) Five specimens with high-strength bond rebar

Fig. 8 Comparison of bond strength between tests and calculations

5. Conclusions

The flexure-shear experiment was conducted on RC beam specimens with the second-layer longitudinal reinforcements cut off, and the behavior of the bond of the second-layer cut-off longitudinal reinforcement was reviewed. Furthermore, the realistic bond-strength reduction coefficient for bond/anchorage failure of the second-layer cut-off longitudinal reinforcement was proposed based on the experimental results. The main conclusions are described below.



- 1) The bond stress of the second-layer cut-off longitudinal reinforcement mostly reached the maximum value, and the bond-splitting failure preceded the maximum strength of the beam specimen for all the specimens as planned.
- 2) Although the strain slope (bond stress) of the second-layer cut-off longitudinal reinforcement increased significantly at the tension-side tip, it started to decrease before the maximum strength of the beam specimen, and the bond deterioration around the second-layer cut-off tip preceded the first-layer longitudinal reinforcement.
- 3) The bond strength of the inner-side reinforcement of the specimen with high-strength bond reinforcement (since yielding did not occur throughout the loading) increased by about 30% compared with the specimen with an equivalent amount of normal-strength reinforcement.
- 4) Regarding the effect of the bond reinforcement on the bond strength, the inside reinforcement improved more than the outside reinforcement.
- 5) The separated-type bond reinforcement (S type) had the same grade of reinforcing effect as the closed-type bond reinforcement (C type).

The relationship between the bond length and bond strength is still mostly unexplained. For example, in the specimen that does not have the second-layer longitudinal reinforcements cut off [5], the bond strength was less than the current bond design equation value. It is considered that the bond-splitting crack is caused by accumulating the bearing-pressure reaction, which acts on each rib of the deformed reinforcing bar in the axial direction. The bond-splitting crack is not caused by just ring tension. Since the reinforcement strength is expected to increase further in the future, further experimentation and analytical research on the bond-splitting strength and its mechanism are required.

6. Acknowledgements

The authors acknowledge the support of the Nuclear and Industrial Safety Agency (NISA) as part of the project on the enhancement of Ageing Management and Maintenance of Nuclear Power Stations and NETUREN for supplying the materials.

7. References

- [1] Architectural Institute of Japan (1999): Design Guideline for Earthquake Resistant Reinforced Concrete Buildings Based on Inelastic Displacement Concept. AIJ, 2nd edition.
- [2] Ayaka Ito, Keisuke Hsegawa, Yuya Zuzuki, Susumu Takahashi, Toshikatsu Ichinose (2013): Splitting bond strength of RC beam which second layer bars cut off. *Journal of Structural and Construction Engineering (Transactions of AIJ)*, **78** (690), 1477-1484.
- [3] Yasuji Shinohara, Kazuhisa Murakami (2014): Bond behaviors of second layer-cutoff bars reinforced by transverse bars having various configurations. *Journal of Structural and Construction Engineering (Transactions of AIJ)*, **79** (706), 1887-1897.
- [4] Architectural Institute of Japan (2010): Recommendation for detailing and placing of concrete reinforcement. AIJ.
- [5] Yasuji Shinohara, Kazuhisa Murakami (2015): Effect of transverse reinforcement on bond splitting behaviors of RC beams with second layer- cutoff bars. *Journal of Structural and Construction Engineering (Transactions of AIJ)*, **80** (714), 1297-1306.